Dalton Transactions

Accepted Manuscript

This article can be cited before page numbers have been issued, to do this please use: C. Gaviglio, J. Pellegrino, D. Milstein and F. Doctorovich, *Dalton Trans.*, 2017, DOI: 10.1039/C7DT03944A.

This is an Accepted Manuscript, which has been through the Royal Society of Chemistry peer review process and has been accepted for publication.

Accepted Manuscripts are published online shortly after acceptance, before technical editing, formatting and proof reading. Using this free service, authors can make their results available to the community, in citable form, before we publish the edited article. We will replace this Accepted Manuscript with the edited and formatted Advance Article as soon as it is available.

You can find more information about Accepted Manuscripts in the author guidelines.

Please note that technical editing may introduce minor changes to the text and/or graphics, which may alter content. The journal's standard Terms & Conditions and the ethical guidelines, outlined in our author and reviewer resource centre, still apply. In no event shall the Royal Society of Chemistry be held responsible for any errors or omissions in this Accepted Manuscript or any consequences arising from the use of any information it contains.

ROYAL SOCIETY OF CHEMISTRY

rsc.li/dalton

View Article Online
DOI: 10.1039/C7DT03944A

$NO^{\bullet}$ Disproportionation by a $\{RhNO\}^9$ Pincer-Type Complex

Carina Gaviglio,[a†] Juan Pellegrino,[b†] David Milstein[c] and Fabio Doctorovich[b,*]

[a]Comisión Nacional de Energía Atómica, CAC-GIyANN, Departamento de Física de la Materia Condensada, Avenida General Paz 1499, San Martín 1650, Buenos Aires, Argentina

[b]Departamento de Química Inorgánica, Analítica, y Química Física, Facultad de Ciencias Exactas y Naturales, Universidad de Buenos Aires. INQUIMAE-CONICET, Ciudad Universitaria, Pab. 2, C1428EHA, Buenos Aires, Argentina

[c]Department of Organic Chemistry, The Weizmann Institute of Science, Rehovot, 76100, Israel

† These authors contributed equally.

Corresponding author´s e-mail address

doctorovich@qi.fcen.uba.ar

Abstract

The reactivity of the $\{RhNO\}^9$ complex $[Rh(PCP^tBu)(NO)]^{\bullet}$ (**1**$^{\bullet}$) with $NO^{\bullet}$ was studied. A disproportionation reaction takes place in which N_2O is released quantitatively, while the complex $Rh(PCP^tBu)(NO)(NO_2)$ (**2**), with coordinated nitrite, is formed. The new complex **2** was fully characterized by multinuclear NMR techniques, IR and X-ray diffraction. The X-ray structure reveals a square pyramidal geometry with an N-bound nitro ligand trans to the C*ipso* of the PCP ligand and a bent nitrosyl ligand in the apical position. IR measurement of released N_2O confirms that one equivalent forms for each molecule of **1**$^{\bullet}$. Infrared spectroscopic experiments with **1**$^{\bullet}$-^{15}NO and $^{14}NO^{\bullet}$ suggest that the reaction occurs through the intermediacy of a dinitrosyl complex. In addition, DFT calculations were performed to provide more evidence on the structure of the intermediates and to support the observed reactivity.

Keywords: nitrosyl, $NO^{\bullet}$ disproportionation, nitro ligand, pincer-type ligand, rhodium, DFT.

View Article Online
DOI: 10.1039/C7DT03944A

Introduction

The coordination chemistry of $NO^{\bullet}$ has been a topic of great interest to inorganic chemists since it was recognized that, unlike other diatomic "simple" ligands such us CO or CN^-, $NO^{\bullet}$ adopts alternative geometries, an aspect related to its redox-active nature.[1,2] Besides this intrinsic significance, nitrosyl complexes have experienced renewed attention since the discovery in the 1980s of the key importance of the nitric oxide radical $NO^{\bullet}$ as a physiologically essential agent.[3] $NO^{\bullet}$ is produced in vivo by the nitric oxide synthase (NOS) family of enzymes and is involved in many important functions such as nerve-signal transduction, vasodilation, blood clotting, and immune response.[3] On the other hand, $NO^{\bullet}$ is also an important intermediate in bacterial and fungal dissimilatory denitrification.[3] In these biological processes, $\{MNO\}^n$ complexes (according to Enemark-Feltham notation)[4,5] are the key intermediates, thus, the coordination chemistry of $NO^{\bullet}$ is a topic of high relevance for an understanding of nitric oxide's biology.[3]

In a recent paper, following a previous work inspired on the idea of a possible "synergistic effect" from the combination of robust bulky pincer ligands with the non-innocence of the NO ligand, we reported the one-electron reduction of the four-coordinate $\{RhNO\}^8$ complex $[Rh(PCP^tBu)(NO)][BF_4]$ (**1**$^+$).[6] The novel $\{RhNO\}^9$ species $[Rh(PCP^tBu)(NO)]^{\bullet}$ (**1**$^{\bullet}$) was well characterized in solution and its reactivity with organic halides was studied, resulting in C-X bond activation; a reactivity that had not been documented for the only previously reported square planar $\{MNO\}^9$ complex, $[Rh(PNP)(NO)]^{\bullet}$ (PNP = $N(^tBu_2PCH_2SiMe_2)_2^-$).[7] This bond activation reactivity reflects the ability of the nitrosyl ligand to act as an electron reservoir. Another aspect of the reactivity of nitrosyl complexes concerns reactions centered at the NO ligand. The chemical transformations of $NO^{\bullet}$ in related NO_x species have long been of interest due to its biological and environmental significance as well as the potential application to selective oxidations of organic substrates.[8] One such reaction is the disproportionation of $NO^{\bullet}$ to nitrous oxide (N_2O) and nitrogen dioxide ($NO_2^{\bullet}$) (eq. 1). There are numerous literature reports describing activation of $NO^{\bullet}$ disproportionation by metal complexes to give N_2O and metal nitrite complexes,[7,9-14] although in one case dinitrogen (N_2) was reported as the reduced product.[7] This disproportionation reaction (eq. 1) is

View Article Online
DOI: 10.1039/C7DT03944A

catalyzed in biological systems by the copper-containing metalloenzyme nitrite reductases.[3] Herein we report the reaction of the $\{RhNO\}^9$ species **1**$^\bullet$ with NO$^\bullet$, which yields N_2O and the five-coordinate nitrosyl complex with nitrite as the fifth ligand, Rh(PCP^{t}Bu)(NO)(NO_2) (**2**). A mechanism is presented which is supported experimentally and by DFT calculations.

$$3\ NO^\bullet \rightarrow NO_2^\bullet + N_2O \qquad (1)$$

Results and discussion

Reaction of [Rh(PCP^{t}Bu)(NO)]$^\bullet$ (1$^\bullet$) upon successive additions of equivalents of NO$^\bullet$ in benzene solution. Formation of Rh(PCP^{t}Bu)(NO)(NO_2) (2). As is shown in Figure 1, upon addition of 1 equiv of NO$^\bullet$ to a benzene solution of **1**$^\bullet$ (black spectrum) the corresponding IR nitrosyl band at 1614 cm^{-1} started to decrease and a shoulder at 1639 cm^{-1} appeared, concomitantly with another IR stretching frequency band at 2218 cm^{-1} (red spectrum). After addition of a second equivalent of NO$^\bullet$ the blue spectrum was registered which shows a more defined band at 1639 cm^{-1} and an increase of the 2218 cm^{-1} band at expenses of a decrese of the band at 1614 cm^{-1}. Full conversion of **1**$^\bullet$ to the new species (ν_{NO} = 1639 cm^{-1}) was observed after addition of a third equivalent of NO$^\bullet$ (green spectrum) while the band at 2218 cm^{-1} increased again. The headspace of this reaction was also monitored by FTIR giving a splitted doublet centered at 2223 cm^{-1}, shown as an inset in Figure 1. This feature was clearly assigned to one of the bands of the IR spectrum of N_2O.[15] The band observed at 2218 cm^{-1} is atributed to N_2O dissolved in benzene.[9]

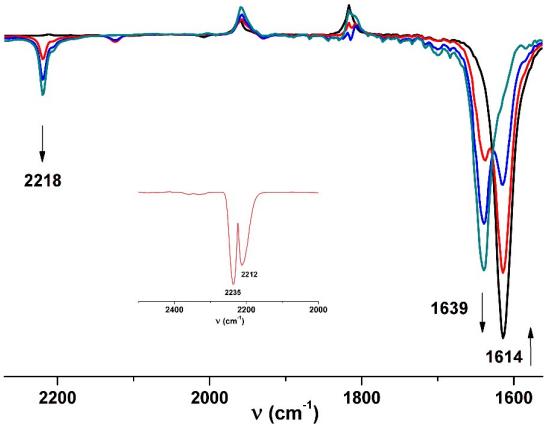

View Article Online
DOI: 10.1039/C7DT03944A

Figure 1. FTIR monitoring of the reaction of **1**• upon successive additions of equivalents of NO• in benzene solution. **1**• (black spectrum), **2** and N_2O dissolved in benzene (green spectrum). Inset: FTIR of the headspace.

Consequently, treatment of complex **1**• with 3 equiv of NO• in benzene solution resulted in quantitative formation of **2** and N_2O (Scheme 1).

SCHEME 1

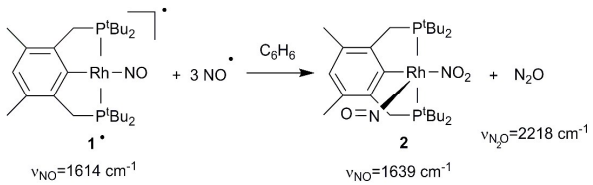

Reaction of the known complex Rh(PCP^{t}Bu)(N_2) (**3**)[16] with NO• also gives **2** quantitatively, through the intermediacy of **1**• (Fig. 2, Scheme 2). Figure 2 shows the IR spectra of solutions of **3** in THF when NO• was incrementally introduced: the band of **1**• at 1614 cm^{-1} and then that of **2** at 1638 cm^{-1} appeared while the intense band of **3** at 2123 cm^{-1} decreased. Also a band at 2223 cm^{-1} increased concomitantly with that of **2**; this feature is assigned to N_2O dissolved in THF.[9] Full conversion is indicated by the last spectrum (green) showing only the bands of **2** and N_2O.

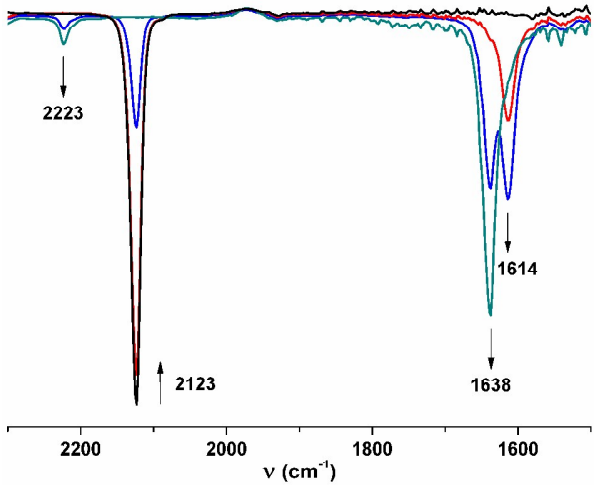

Figure 2. FTIR monitoring of the reaction of **3** upon successive additions of equivalents of NO• in THF solution. **3** (black spectrum), **1**• and **3** (red spectrum), **2** and N_2O dissolved in THF (green spectrum).

View Article Online
DOI: 10.1039/C7DT03944A

SCHEME 2

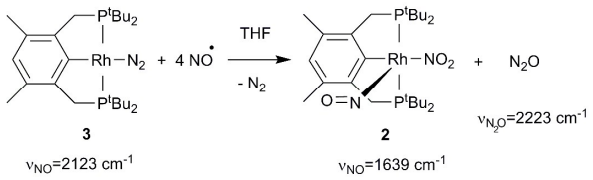

Somehow surprisingly, the disproportionation reaction of NO$^\bullet$ in the case of the closely related pincer complex [Rh(PNP)(NO)]$^\bullet$ was reported to yield dinitrogen as the reduced product of NO$^\bullet$,[7] instead of N_2O, which is the reduced product detected in our case and in the NO$^\bullet$ disproportionation reaction with many other transition-metal complexes.[9-14]

The appearance of N_2O and **2** after addition of approximately only 1 equivalent of NO$^\bullet$ to **1**$^\bullet$ indicates fast reaction kinetics, where any intermediate, such as a dinitrosyl complex, reacts quickly with NO$^\bullet$ to afford **2**. In the same way, the observation of the isosbestic point around 1630 cm^{-1} in the IR spectra of solutions of **1**$^\bullet$ when NO$^\bullet$ was incrementally introduced (Figure 1), also suggests a clean and rapid conversion of reactant to product, with no build-up of any intermediates.

Although such rapid reactivity precludes the spectroscopic detection of an intermediate, it is likely that a transient dinitrosyl complex, $Rh(NO)_2$, or hyponitrito species, $Rh(N_2O_2)$, forms. Both have been previously postulated in proposed mechanisms for NO$^\bullet$ reduction to N_2O.[7,9-13] Very recently Karlin and coworkers reported that a copper complex, $[Cu^I(tmpa)(MeCN)]^+$ (TMPA = tris(2-pyridylmethyl)amine), reductively couples NO$^\bullet$ in methanol, giving a structurally characterized hyponitritodicopper(II) adduct. Interestingly, while this adduct is stable in MeOH (the authors suggest that H-bonding to the hyponitrite moiety is crucial for the stabilization), it disproportionates when dissolved in THF, leading to a Cu^{II} nitrite complex and N_2O.[17] In other outstanding work, it has been reported that ferrous ions in Fe^{2+}-exchanged MOF-5 disproportionate nitric oxide to produce nitrous oxide and a ferric nitrito complex through the intermediacy of a ferric hyponitrite radical, $Fe^{III}(N_2O_2^{\bullet-})$.[18] Remarkably this study provided the first evidence for a monoanionic hyponitrite radical metal complex as the active intermediate in the metal-mediated NO$^\bullet$

View Article Online
DOI: 10.1039/C7DT03944A

disproportionation. It is worth mentioning that the uncoordinated hyponitrite radical, $N_2O_2^{\bullet-}$, has been detected as a transient species and reacts with $NO^{\bullet}$ to give the nitrosyl hyponiotrite radical, $N_3O_3^{\bullet-}$, that rapidly decomposed in N_2O and NO_2^-.[19,20]

Mixed-labeling experiments provide indirect evidence for the intermediacy of a dinitrosyl complex in our system. The same strategy was previously used to prove the intermediacy of dinitrosyl complexes as intermediates in $NO^{\bullet}$ disproportionation mediated by manganese and iron tropocoronand complexes[9,10] and manganese porphyrinates.[13] The black spectrum in Figure 3 corresponds to $[Rh(PCP)(^{15}NO)]^{\bullet}$ (**1**$^{\bullet}$-^{15}NO), with a strong band at 1581 cm^{-1}. Exposure of a benzene solution of **1**$^{\bullet}$-^{15}NO to one equivalent of $^{14}NO^{\bullet}$ led to the formation of a new band at 1612 cm^{-1} together with an incipient absorbance around 1640 cm^{-1}. After the addition of a second equivalent of $^{14}NO^{\bullet}$ these features continued to increase in intensity at the expense of the 1581 cm^{-1} band of **1**$^{\bullet}$-^{15}NO. Finally, when approximately 3 equivalents of $^{14}NO^{\bullet}$ were added, the 1581 cm^{-1} band was almost completely lost, and the absorbance at 1640 cm^{-1} increased while the feature at 1612 cm^{-1} decreased slightly reaching a 3:1 intensity relation approximately. The band at 1640 cm^{-1} corresponds to the nitrite complex $Rh(PCP)(^{14}NO)(NO_2)$ (**2**-^{14}NO) (Scheme 1), while the band at 1612 cm^{-1} is attributed to its **2**-^{15}NO counterpart. On the other hand, the peaks at 2219, 2196, 2173 and 2150 cm^{-1}, that increased upon the incremental addition of ^{14}NO (Figure 3, inset), are assigned to $^{14}N_2O$, $^{14}N^{15}NO$, $^{15}N^{14}NO$ and $^{15}N_2O$, respectively.[21] The binding of $NO^{\bullet}$ in **1**$^{\bullet}$ is irreversible ($NO^{\bullet}$ if not lost under vacuum and is not displaced by trimethylphosphine), so the complete scrambling of labels in the formation of N_2O, could be explained as the result of the formation of a dinitrosyl complex in equilibrium with the mononitrosyl, as shown in Scheme 3. From the spectra in Figure 3 it can be seen that **1**$^{\bullet}$-^{14}NO is indeed formed, as it should be according to the equilibrium represented in Scheme 3. The band of **1**$^{\bullet}$-^{14}NO appears at 1614 cm^{-1} (Figure 1), so it is mixed with the one attributed to **2**-^{15}NO (1612 cm^{-1} in Figure 3).

SCHEME 3

View Article Online
DOI: 10.1039/C7DT03944A

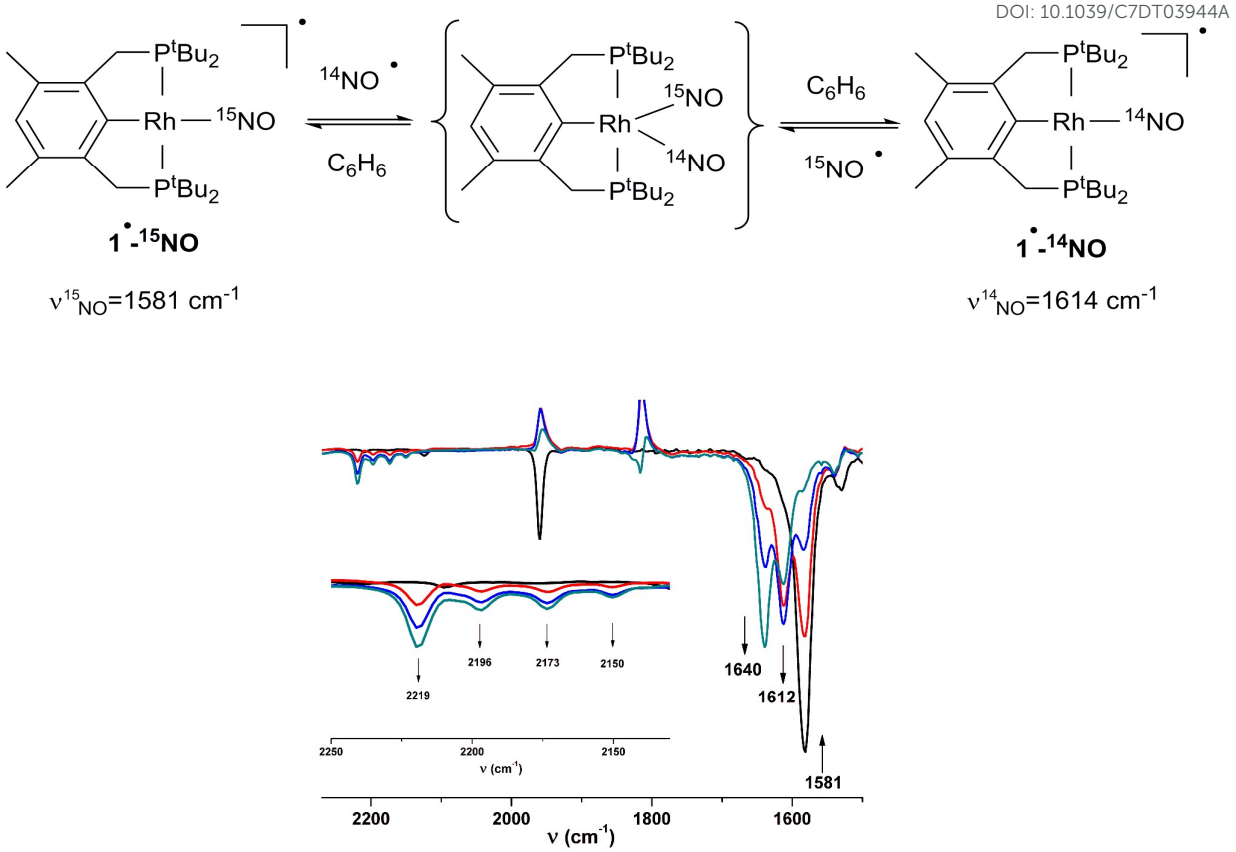

Figure 3. FTIR monitoring of the reaction of **1**$^{\bullet}$-^{15}NO upon successive additions of equivalents of ^{14}NO in benzene solution. Inset: enlargement of the bands attributed to the N_2O isotopomers. **1**$^{\bullet}$-^{15}NO (black spectrum); **2**-^{14}NO, **2**-^{15}NO and N_2O isotopomers (green spectrum).

Finally, we tested the addition of NO$^{\bullet}$ to a solution of isolated **2**, to check if N_2O can be produced, since **2** could lose $NO_2^{\bullet}$ in the presence of excess NO$^{\bullet}$ to give the intermediate dinitrosyl complex, that would further react to generate N_2O and **2** again. If this happened, NO$^{\bullet}$ disproportation to produce N_2O and $NO_2^{\bullet}$ would occur under catalytic conditions, as in the case of the Fe tropocoronand complex reported by Lippard and coworkers.[10] However, treatment of **2** with NO$^{\bullet}$ did not produce N_2O, so this reaction pathway is not operating in our case, which means that $NO_2^{\bullet}$ is irreversible bound in **2**. Indeed, during the mixed-labeling experiments we observed that **2**-^{15}NO, slowly converts to **2**-^{14}NO under excess ^{14}NO$^{\bullet}$, which indicates that **2** loses NO$^{\bullet}$ more easily than $NO_2^{\bullet}$.

View Article Online
DOI: 10.1039/C7DT03944A

Reaction of [Rh(PCP^{t}Bu)(NO)][BF_4] (1^+) with $NaNO_2$. Formation of Rh(PCP^{t}Bu)(NO)(NO_2) (2). The identity of **2** as the complex Rh(PCP)(NO)(NO_2) was confirmed by its independent preparation. Reaction of [Rh(PCP)(NO)][BF_4] ($\mathbf{1}^+$)[22] with sodium nitrite in a dichloromethane-methanol mixture gave **2** after stirring for some minutes (Scheme 4). Complex **2** was fully characterized including X-ray structure determination.

SCHEME 4

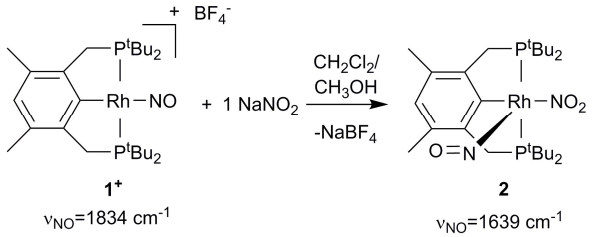

The new complex **2** was fully characterized by multinuclear NMR techniques, FTIR and X-ray diffraction. The $^{31}P\{^1H\}$ NMR spectrum of **2** (Figure S1) exhibits a doublet at δ 77.4 ppm with a $^1J_{Rh,P}$ of 145.7 Hz, indicating two equivalent phosphorus nuclei coordinated to a rhodium center. The chemical shift and coupling constant are very similar to the ones reported for other five-coordinate $\{RhNO\}^8$ complexes.[22] The IR spectrum as is shown in Figure 1 displays a diagnostic signal for ~~bent~~ NO at 1639 cm^{-1} in benzene solution. The possible bands ascribed to the coordinated nitrite ligand were not evident; they are probably masked by ligand absorptions. The molecular structure of **2** was confirmed by an X-ray diffraction study of single crystals obtained by slow evaporation from a concentrated solution of **2** in dichloromethane at room temperature (Figure 4). Selective bond lengths and bond angles are given in Table 1. The rhodium atom is located in the center of a square-pyramid with a bent apical nitrosyl group occupying the position *trans* to the empty coordination site and N-bound NO_2 *trans* to the *ipso* carbon. The rhodium atom in complex **2** can be described as Rh(III) with a Rh-N(1)-O(1) angle of 125.46(17)º, confirming the bent NO character of the nitrosyl ligand, and a N(1)-O(1) bond distance of 1.171(3) Å, both in the range observed for similar pentacoordinated pincer-type rhodium nitrosyl complexes.[22]

View Article Online
DOI: 10.1039/C7DT03944A

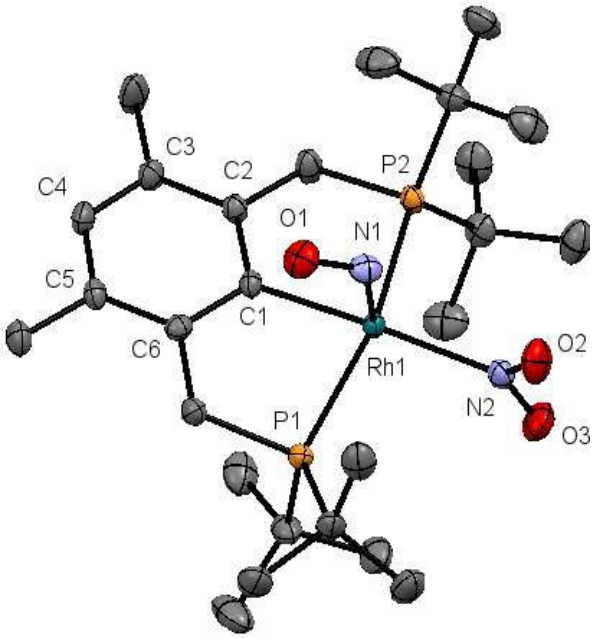

Figure 4. ORTEP plot of complex **2** at 50% probability level. Hydrogen atoms are omitted for clarity.

TABLE 1. Selected bond lengths (Å) and angles (deg) for 2

Rh(1)-N(1)	1.907(2)	N(2)-O(3)	1.241(3)
Rh(1)-N(2)	2.1515(19)	C(1)-C(2)	1.404(3)
Rh(1)-C(1)	2.069(2)	C(2)-C(3)	1.406(3)
Rh(1)-P(1)	2.3234(6)	C(3)-C(4)	1.387(3)
Rh(1)-P(2)	2.3765(6)	C(4)-C(5)	1.388(3)
N(1)-O(1)	1.171(3)	C(5)-C(6)	1.397(3)
N(2)-O(2)	1.240(3)	C(6)-C(1)	1.419(3)
Rh(1)-N(1)-O(1)	125.46(17)	N(2)-Rh(1)-C(1)	177.42(8)
N(1)- Rh(1)-N(2)	91.08(8)	P(1)-Rh(1)-C(1)	81.37(6)

View Article Online
DOI: 10.1039/C7DT03944A

N(1)-Rh(1)-P(1)	98.26(6)	P(2)-Rh(1)-C(1)	82.08(6)
N(1)-Rh(1)-P(2)	99.49(6)	P(1)-Rh(1)-N(2)	96.61(5)
N(1)-Rh(1)-C(1)	90.79(9)	P(2)-Rh(1)-N(2)	99.35(5)
P(2)-Rh(1)-P(1)	155.81(2)		

Mechanism

The following mechanism is proposed to explain the observed reactivity for **1**$^{\bullet}$ towards successive additions of equivalents of NO$^{\bullet}$.

SCHEME 5

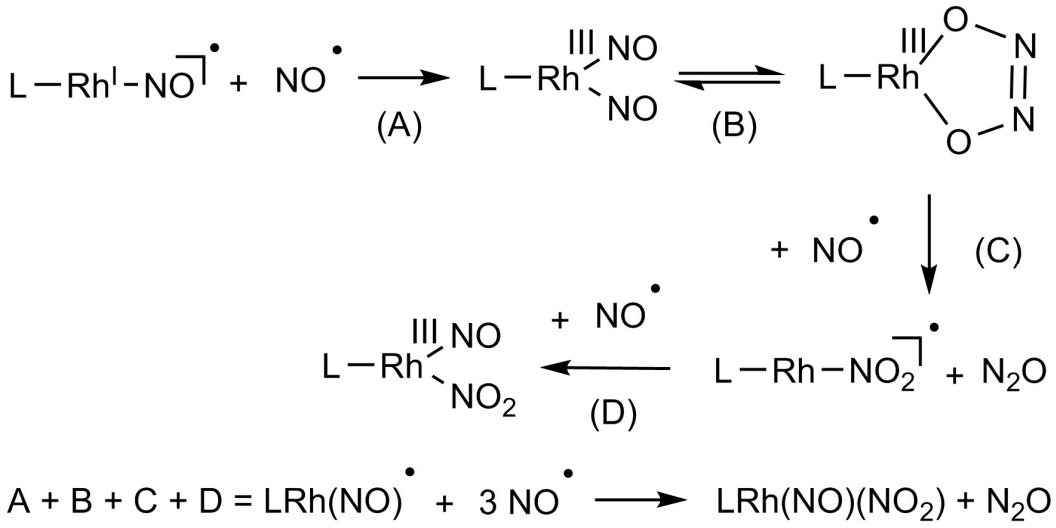

The calculated reaction energies for the three steps A, C and D are favorable: -21, -47 and -39 kcal/mol, respectively. The energy involved in reaction A is around the entropy penalty while the one for the reaction D is larger, so they are both possible. The calculated reaction energy for B is near 0 and for the global reaction (A + B + C+ D) is -107 kcal/mol.

We also performed DFT optimizations for different forms of the unobserved dinitrosyl reactive intermediate. Three possible isomers were considered: Rh(PCP)(η^2-N_2O_2) (Figure S5), Rh(PCP)(NO)(NO) and Rh(PCP)(κ^2-ONNO) (Figure 5).

View Article Online
DOI: 10.1039/C7DT03944A

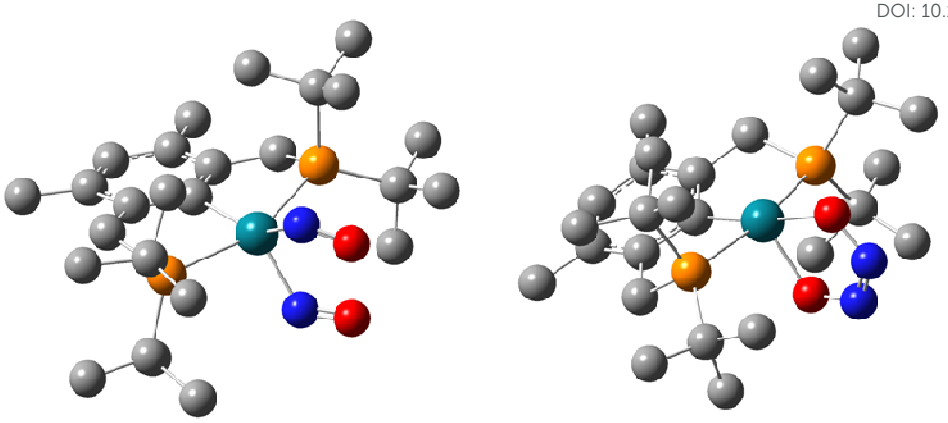

Figure 5. DFT-optimized structures of (PCP)Rh(NO)(NO) and (PCP)Rh(κ^2-ONNO) (hydrogen atoms are omitted).

The energies of Rh(PCP)(NO)(NO) and Rh(PCP)(κ^2-ONNO) are comparable, and around 20 kcal/mol below that of Rh(PCP)(η^2-N_2O_2). On the other hand, they are around 21 kcal/mol below the sum of the energies of Rh(PCP)(NO)$^\bullet$ and free NO$^\bullet$ so they seem to be plausible structures for the reactive intermediate. The calculated Rh(PCP)(κ^2-ONNO) structure shows similar N-O and N-N bonds to the ones reported for the few X-ray structures of κ^2-ONNO complexes,[23] though differently from the reported systems, the ONNO ligand is not coordinated in a symmetric fashion (one Rh-O distance is 2.00 Å and the other one is 2.14 Å while one C-Rh-O angle is 109.7 and the other one is 173.3º). On the other hand, while the Rh(PCP)(η^2-N_2O_2) structure is best described as a neutral N_2O_2 ligand coordinated to a rhodium(I) center, Rh(PCP)(κ^2-ONNO) is clearly a rhodium(III) hyponitrite complex (much longer N-O distances). Also, the dinitrosyl complex is described as a rhodium(III) center coordinated to two NO^- ligands (both Rh-N-O angles are around 125º). Based on the relative energies of these forms of the intermediate, the addition of one equivalent of NO$^\bullet$ to **1**$^\bullet$ could afford either a dinitrosyl or a hyponitrito intermediate. Then a second molecule of NO$^\bullet$ would react with this species to yield N_2O and paramagnetic Rh(PCP)(NO_2)$^\bullet$ that rapidly traps another NO$^\bullet$ molecule to give the final product Rh(PCP)(NO)(NO_2). From the mixed-labeling experiments, it can be concluded that a dinitrosyl complex Rh(PCP)(NO)(NO) is formed. Interestingly, attempts to optimize a complex with the N_3O_3 moiety coordinated to rhodium (the radical $N_3O_3^{\bullet-}$ was detected as a transient species in the free form)[19,20] failed, the optimization converged to the paramagnetic

View Article Online
DOI: 10.1039/C7DT03944A

$Rh(PCP)(NO_2)^{\bullet}$ and free N_2O. On the other hand, optimization of complexes with separated NO and N_2O_2 moieties resulted in stationary points (two of them are shown in Figure S6). One of the structures is a rhodium(III) complex with bent NO^- and a hyponitrite radical ligand, $Rh^{III}(NO^-)(N_2O_2^{\bullet-})$. This intermediate would then react with another equivalent of $NO^{\bullet}$ to yield the final products $Rh(PCP)(NO_2)(NO)$ (**2**) and N_2O without the intermediacy of $Rh(PCP)(NO_2)^{\bullet}$**.** However, all the forms proposed for this intermediate resulted quite high in energy (20 kcal/mol) with respect to $Rh(PCP)(NO_2)^{\bullet}$ and N_2O, so probably this route is not competitive with the one proposed in Scheme 5.

Reaction of $[Rh(PCP^tBu)(NO)]^{\bullet}$ ($1^{\bullet}$) with O_2 in benzene solution. Formation of $Rh(PCP^tBu)(NO)NO_2$ (2) and $Rh(PCP^tBu)O_2$. We tried the reaction of $\mathbf{1}^{\bullet}$ with O_2, that could give the paramagnetic $Rh(PCP)(NO_2)^{\bullet}$ complex, proposed as an intermediate in the mechanism of $NO^{\bullet}$ disproportionation by $\mathbf{1}^{\bullet}$. However, the reaction of $\mathbf{1}^{\bullet}$ with O_2 gave a mixture of **2** and the known oxygen complex $Rh(PCP)(O_2)$[24] (Scheme 6), as judged by IR and ^{31}P NMR (Figure S4), along with a species derived from the free ligand (probably a phosphine oxide).

SCHEME 6

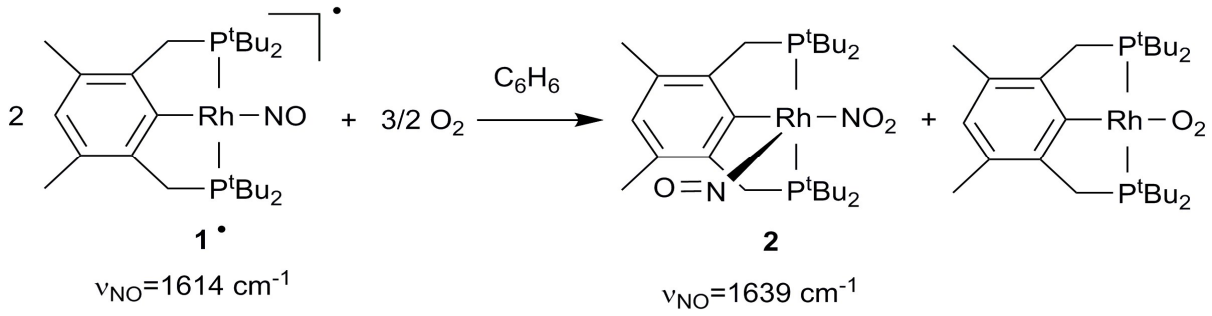

We propose the following sequence of reactions to explain this reactivity.

SCHEME 7

View Article Online
DOI: 10.1039/C7DT03944A

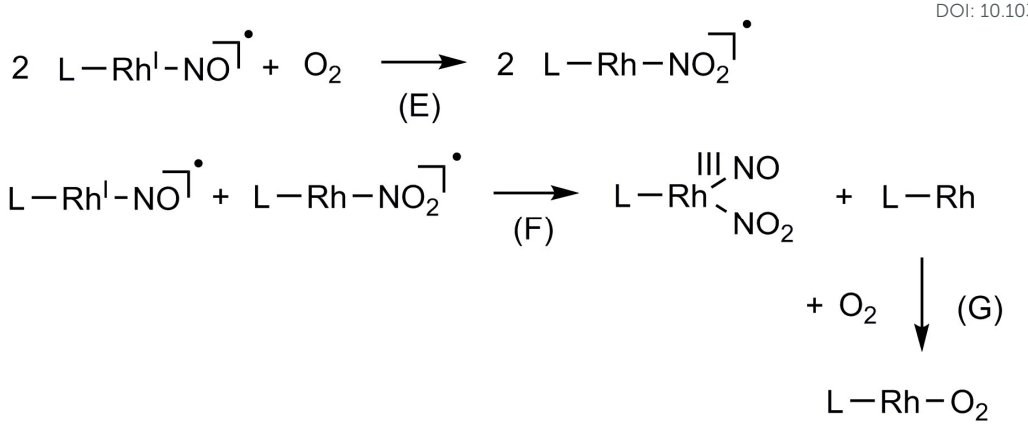

The calculated reaction energies for the three steps are favorable: -58, -2 and -23 kcal/mol for reactions E, F and G, respectively. Probably reaction F that involves two reacting complexes is not operating due to the steric bulk provided by the two phosphines and instead generated free $NO_2^{\bullet}$ reacts with **1**$^{\bullet}$ to give **2**. Reaction E could occur through the intermediacy of a reactive species such as peroxinitrite[25-27] that ultimately gives $NO_2^{\bullet}$ (free or coordinated) and other oxidized species such as the phosphine oxide derived from the PNP ligand.

Finally, we also studied the reaction of **2** with substrates that could participate in O-transfer reactions, such as phosphines or alkenes that could be attacked by the nitrite ligand in **2** to give the phosphine oxide or the epoxide respectively. This reactivity was previously reported for some nitrite complexes.[28,29] However, **2** did not react at all with excess of these kind of substrates (trimethylphosphine and cycloctene were tried), even upon heating at 85ºC overnight.

Experimental

1. Syntheses. All experiments with metal complexes and phosphine ligands were carried out under an atmosphere of purified nitrogen in a MBraun glovebox or using standard Schlenk techniques under argon atmosphere. All solvents were analytical grade or better. CH_2Cl_2 was distilled over calcium hydride under nitrogen. All other solvents were refluxed over sodium/benzophenone ketyl and distilled under nitrogen. Commercially available reagents were used as received. NO$^{\bullet}$ was

View Article Online
DOI: 10.1039/C7DT03944A

generated by the reaction between $NaNO_2$ and $FeSO_4.7H_2O$ and stored over KOH at atmospheric pressure.

2. Physical measurements. IR spectra were obtained using a Nicolet Avatar FTIR spectrophotometer. ^1H, ^{13}C, and ^{31}P NMR spectra were recorded using a Bruker 500 MHz NMR spectrometer. ^1H and $^{13}C\{^1H\}$ NMR chemical shifts are reported in ppm downfield from tetramethylsilane. ^1H NMR chemical shifts were referenced to the residual hydrogen signal of the deuterated solvent (7.15 ppm, benzene; 5.32 ppm, dichloromethane). In $^{13}C\{^1H\}$ NMR measurements the signals of deuterated benzene (128.0 ppm), or deuterated dichloromethane (53.8 ppm), were used as a reference. ^{31}P NMR chemical shifts were reported in ppm downfield from H_3PO_4 and referenced to an external 85% solution of phosphoric acid in D_2O. Abbreviations used in the description of NMR data are as follows: br, broad; s, singlet; d, doublet; t, triplet; q, quartet; m, multiplet; v, virtual.

3. Computational methodology. All calculations were carried out with the program package Gaussian03.[30] The structures of all molecules were fully geometry optimized at DFT level, using the PBE exchange-correlation functional. The LANL2DZ basis set and pseudo potential were used for the rhodium atom. For the H, N, O, C and P atoms 6-31G** basis set was used, The vibrational frequencies were calculated on optimized structures using the same functional and basis set.

Reaction of [Rh(PCP^{t}Bu)(NO)]$^\bullet$ (1$^\bullet$) with NO$^\bullet$ in benzene solution. Formation of Rh(PCP^{t}Bu)(NO)(NO$_2$) (2). Treatment of complex **1$^\bullet$** (10 mg, 0.018 mmol), prepared as previously described,[6] with 3 equiv of NO$^\bullet$ in benzene solution resulted in quantitative formation of **2** and N_2O. 1 mL of headspace was introduced into a gas cell with a path length of 5 cm for FTIR detection. For comparison, the headspace of a solution of the HNO donor N-hydroxy-4-nitro benzene sulfonamide[31,32] at pH 12 was measured under the same conditions, giving the same signal with an intensity proportional to the expected amount of generated N_2O. Single crystals suitable for X-ray diffraction were obtained by crystallization from a concentrated solution of **2** in dichloromethane at room temperature.

View Article Online
DOI: 10.1039/C7DT03944A

Characterization of 2: $^{31}P\{^{1}H\}$ NMR (C_6D_6): 77.40 (d, $^{1}J_{RhP}$ = 145.7 Hz). ^{1}H NMR (CD_2Cl_2): 6.67 (s, 1H, Rh-***Ar***), 3.05 (AB quartet, $^{2}J_{HH}$ = 19.9 Hz, 4H, Ar-C***H***$_2$-P), 2.17 (s, 6H, 2 Ar-C***H***$_3$), 1.13 (vt, J_{PH} = 6.7 Hz, 18H, 2 (C***H***$_3$)$_3$C-P), 0.93 (vt, J_{PH} = 6.8 Hz, 18H, 2 (C***H***$_3$)$_3$C-P). $^{13}C\{^{1}H\}$ NMR (C_6D_6): 165.15 (d, $^{2}J_{RhC}$ = 34.8 Hz, C_{ipso}, Rh-***Ar***), 145.30 (vtd, J_{PC} = 8.2 Hz, J_{RhC} = 1.5 Hz, Rh-***Ar***), 130.77 (vtd, J_{PC} = 7.9 Hz, , $^{2}J_{RhC}$ = 1.2 Hz, Rh-***Ar***), 128.72 (s, C_{para},Rh-***Ar***), 36.81 (vtd, J_{PC} = 7.5 Hz, $^{2}J_{RhC}$ = 1.1 Hz, $(CH_3)_3$***C***-P), 35.42 (vtd, J_{PC} = 7.4 Hz, $^{2}J_{RhC}$ = 0.9 Hz, $(CH_3)_3$***C***-P), 30.82 (vtd, J_{PC} = 11.2 Hz, $^{2}J_{RhC}$ = 2.0 Hz, Ar-***C***H_2-P), 30.31 (vt, J_{PC} = 2.4 Hz, (***C***H_3)$_3$C-P), 28.38 (vt, J_{PC} = 2.1 Hz, (***C***H_3)$_3$C-P), 22.31 (s, ***C***H_3-Ar), (assignment of $^{13}C\{^{1}H\}$ NMR signals was confirmed by ^{13}C DEPT135). IR ν (C_6H_6; cm^{-1}): 1639 (s, NO). Anal. Calcd: C, 52.00; H, 7.89. Found: C, 52.21; H, 7.91.

X-ray Structural Analysis of 2. *Crystal data:* $C_{26}H_{47}N_2O_3P_2Rh$, brown, prism, 0.60 x 0.20 x 0.10 mm^3, monoclinic; *P* 1 21/n 1; *a* = 8.6789(2) Å, *b* = 23.1826(5)Å, *c* = 14.3797(3) Å; β = 94.098(2)°, from 25 degrees of data; *T* = 170(2) K; *V* = 2885.79(12) $Å^3$, *Z* = 4; Fw = 600.50; D_c = 1.382 g/cm^3; μ = 0.731 mm^{-1}. *Data Collection and Processing:* Oxford Gemini E CCD area detector diffractometer, Mo Kα (λ = 0.71073 Å), graphite monochromator; $-11 \le h \le 11$, $-30 \le k \le 29$, $-18 \le l \le 19$, 62794 reflections collected, 7231 independent reflections (R_{int} = 0.0743). For data collection, cell refinement and data reduction CrysAlisPro software was used. Absorption correction was made by multi-scan. *Solution and Refinement:* The structure was solved by direct methods with SHELXT. Full-matrix least-squares refinement based on F^2 with SHELXL; 321 parameters with 0 restraints, final R_1 = 0.0337 (based on F^2) for data with $I > 2\ \sigma\ (I)$. and R_1 = 0.0573 on 7231 reflections, goodness-of-fit on F^2 = 1.126 , largest electron density peak = 0.834 e $Å^{-3}$.

Reaction of Rh(PCP^{t}Bu)(N_2) (3) with NO$^\bullet$ in THF solution. Formation of Rh(PCP^{t}Bu)(NO)NO_2 (2). NO$^\bullet$ was bubbled to a solution of complex **3**[16] (15 mg, 0.027 mmol) in THF. The reaction was monitored by IR, after full conversion the solvent was removed in vacuo. The solid was redissolved in THF and ^{31}P NMR revealed quantitative formation of **2**.

View Article Online
DOI: 10.1039/C7DT03944A

Reaction of [Rh(PCP^{t}Bu)(NO)]$^\bullet$ ($\mathbf{1^\bullet}$) with O_2 in benzene solution. Formation of Rh(PCP^{t}Bu)(NO)NO_2 (2). Treatment of complex $\mathbf{1^\bullet}$ (10 mg, 0.018 mmol), with approximately 3 equiv of O_2 in benzene solution resulted in the formation of **2**, Rh(PCP)(O_2), and some oxidized ligand, as judged by ^{31}P NMR and IR.

Reaction of [Rh(PCP^{t}Bu)(NO)][BF_4] ($\mathbf{1^+}$) with $NaNO_2$. Formation of Rh(PCP^{t}Bu)(NO)NO_2 (2). Dichloromethane (1 mL) and methanol (0.5 mL) were added to a mixture of solid $\mathbf{1^+}$ (16 mg, 0.025 mmol), prepared as previously described,[6,22] and solid $NaNO_2$ (2.1 mg, 0.030 mmol). The suspension was stirred at room temperature for some minutes resulting in a color change from green to brown. $^{31}P\{^1H\}$ NMR revealed quantitative formation of **2** as a single new product. The solvent was evaporated and the remaining solid was extracted with toluene. Evaporation of toluene under vacuum gave 13.8 mg of **2** in 92 % yield.

Conclusions

The reaction of $\mathbf{1^\bullet}$ with NO$^\bullet$ was studied. A NO$^\bullet$ disproportionation reaction took place yielding the nitrite nitrosyl complex **2** and free N_2O, while no intermediates could be detected. Anyway, a mechanism was proposed, supported by DFT calculations.

The crystallographic characterization of the nitrite complex revealed a N-nitrite coordination as observed in the analogous complex Rh(PNP)(NO)(NO_2). The nitrite complex did not participate in O-transfer reactions with phosphines or alkanes.

Conflicts of interest

There are no conflicts to declare.

View Article Online
DOI: 10.1039/C7DT03944A

Acknowledgements

This work was financially supported by the University of Buenos Aires (UBACYT 20020130100642BA), ANPCyT (PICT 2014-1278). CG, JP and FD are CONICET members. DM holds the Israel Matz Professorial Chair of Organic Chemistry.

Notes and references

1. D. M. P. Mingos, in *Nitrosyl Complexes in Inorganic Chemistry, Biochemistry and Medicine I*, Springer, Berlin, Germany, 2014, 153, 1-44.

2. F. Roncaroli, M. Videla, L. D. Slep and J. A. Olabe, *Coord. Chem. Rev.*, 2007, **251**, 1903-1930.

3. L. E. Goodrich, F. Paulat, V. K. K. Praneeth and N. Lehnert, *Inorg. Chem.*, 2010, **49**, 6293-6316.

4. R. D. Feltham and J. H. Enemark, *Topics Stereochem.*, 1981, **12**, 155-215.

5. J. H. Enemark and R. D. Feltham, *Coord. Chem. Rev.*, 1974, **13**, 339-406.

6. J. Pellegrino, C. Gaviglio, D. Milstein and F. Doctorovich, *Organometallics*, 2013, **32**, 6555-6564.

7. A. Y. Verat, M. Pink, H. Fan, B. C. Fullmer, J. Telser and K. G. Caulton, *Eur. J. Inorg. Chem.*, 2008, **30**, 4704-4709.

8. Y. Jiang and H. Berke, in *Nitrosyl Complexes in Inorganic Chemistry, Biochemistry and Medicine I*, Springer, Berlin, Germany, 2013, 153, 167-228.

9. K. J. Franz and S. L. Lippard, *J. Am. Chem. Soc.*, 1998, **120**, 9034-9040.

10. K. J. Franz and S. L. Lippard, *J. Am. Chem. Soc.*, 1999**, 121**, 10504-10512.

11. K. M. Miranda, X. Bu, I. Lorkovic and P. C. Ford, *Inorg. Chem.*, 1997, **36**, 4838-4848.

View Article Online
DOI: 10.1039/C7DT03944A

12. I. M. Lorkovic´ and P. C. Ford, *Inorg. Chem.*, 1999, **38**, 1467-1473.

13. G. G. Martirosyan, A. S. Azizyan, T. S. Kurtikyan, P. C. Ford, P. C. *Inorg. Chem.*, 2006, **45**, 4079.

14. S. Ghosh, H. Deka, Y. B. Dangat, S. Saha, K. Gogoi, K. Vankab and B. Mondal, *Dalton Trans.*, 2016, **45**, 10200-10208.

15. D. E. Burch and D. Williams, *Appl. Opt.*, 1962, **1**, 473-482.

16. A. Vigalok and D. Milstein, *Organometallics*, 2000, **19**, 2061-2064.

17. G. B. Wijeratne, S. Hematian, M. A. Siegler and K. D. Karlin, *J. Am. Chem. Soc.* 2017, **139** (38), 13276-13279.

18. C. K. Brozek, J. T. Miller, S. A. Stoian and M. Dincă, *J. Am. Chem. Soc.*, 2015, **137**, 7495-7501.

19. M. Valiev and S. V. Lymar, *J. Phys. Chem. A* 2011, **115,** 12004-12010.

20. V. Shafirovich and S. V. Lymar, *Proc. Natl. Acad. Sci. U.S.A.* 2002, **99**, 7340-7345.

21. A. Lapinski, J. Spanget-Larsen, J. Waluk and J. Radziszewski, *J. Chem.Phys.* 2001, **115**, 1757-1764.

22. C. Gaviglio, Y. Ben-David, L. J. W. Shimon, F. Doctorovich and D. Milstein, *Organometallics*, 2009, **28**, 1917-1926.

23. Wright, A. M.; Wu, G.; Hayton, T. W. *J. Am. Chem. Soc.* **2012**, *134*, 9930-9933.

24. C. M. Frech, L. J. W. Shimon and D. Milstein, *Helv. Chim. Acta*, 2006, **89**, 1730-1739.

25. T. S. Kurtikyan, Sh. R. Eksuzyan, V. A. Hayrapetyan, G. G. Martirosyan, G. S. Hovhannisyan, J. A. Goodwin, *J. Am. Chem. Soc.*, 2012, **134**, 13861-13870.

View Article Online
DOI: 10.1039/C7DT03944A

26. G. Y. Park, S. Deepalatha, S. C. Puiu, D. H. Lee, B. Mondal, A. A. N. Sarjeant, D. del Rio, M. Y. M. Pau, E. I. Solomon and K. D. Karlin, *J. Biol. Inorg. Chem.*, 2009, **14**, 1301-1311.

27. C. M. Frech, O. Blacque, H. W. Schmalle and H. Berke, *Dalton Trans.*, 2006, 4590-4598.

28. J. Heinecke and P. C. Ford, *J. Am. Chem. Soc.*, 2010, **132**, 9240-9243.

29. C. Khin, J. Heinecke and P. C. Ford. *J. Am. Chem. Soc.* 2008, **130**, 13830-13831.

30. Gaussian 03, Revision C.02, M. J. Frisch, G. W. Trucks, H. B. Schlegel, G. E. Scuseria, M. A. Robb, J. R. Cheeseman, J. A. Montgomery, Jr., T. Vreven, K. N. Kudin, J. C. Burant, J. M. Millam, S. S. Iyengar, J. Tomasi, V. Barone, B. Mennucci, M. Cossi, G. Scalmani, N. Rega, G. A. Petersson, H. Nakatsuji, M. Hada, M. Ehara, K. Toyota, R. Fukuda, J. Hasegawa, M. Ishida, T. Nakajima, Y. Honda, O. Kitao, H. Nakai, M. Klene, X. Li, J. E. Knox, H. P. Hratchian, J. B. Cross, V. Bakken, C. Adamo, J. Jaramillo, R. Gomperts, R. E. Stratmann, O. Yazyev, A. J. Austin, R. Cammi, C. Pomelli, J. W. Ochterski, P. Y. Ayala, K. Morokuma, G. A. Voth, P. Salvador, J. J. Dannenberg, V. G. Zakrzewski, S. Dapprich, A. D. Daniels, M. C. Strain, O. Farkas, D. K. Malick, A. D. Rabuck, K. Raghavachari, J. B. Foresman, J. V. Ortiz, Q. Cui, A. G. Baboul, S. Clifford, J. Cioslowski, B. B. Stefanov, G. Liu, A. Liashenko, P. Piskorz, I. Komaromi, R. L. Martin, D. J. Fox, T. Keith, M. A. Al-Laham, C. Y. Peng, A. Nanayakkara, M. Challacombe, P. M. W. Gill, B. Johnson, W. Chen, M. W. Wong, C. Gonzalez and J. A. Pople, Gaussian, Inc., Wallingford CT, 2004.

31. K. Sirsalmath, S. A. Suárez, D. E. Bikiel and F. Doctorovich, *J. Inorg. Biochem.*, 2013, **118**, 134-139.

32. L. De Luca Porcheddu and G. Giacomelli, *Syn. Lett*, 2009, **13**, 2149-2153.

View Article Online
DOI: 10.1039/C7DT03944A

TOC

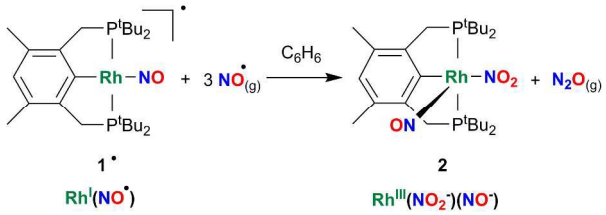

NO$^\bullet$ disproportionation by the pincer-type complex [Rh(PCP^{t}Bu)(NO)]$^\bullet$ (**1**$^\bullet$) results in the formation of Rh(PCP^{t}Bu)(NO)(NO$_2$) (**2**) with coordinated nitrite and quantitative release of N_2O.